nature biotechnology

FOCUS | REVIEW ARTICLE

https://doi.org/10.1038/s41587-019-0198-8

Next-generation interfaces for studying neural function

James A. Frank[1,2], Marc-Joseph Antonini[1,2,3] and Polina Anikeeva[1,2,4*]

Monitoring and modulating the diversity of signals used by neurons and glia in a closed-loop fashion is necessary to establish causative links between biochemical processes within the nervous system and observed behaviors. As developments in neural-interface hardware strive to keep pace with rapid progress in genetically encoded and synthetic reporters and modulators of neural activity, the integration of multiple functional features becomes a key requirement and a pressing challenge in the field of neural engineering. Electrical, optical and chemical approaches have been used to manipulate and record neuronal activity in vivo, with a recent focus on technologies that both integrate multiple modes of interaction with neurons into a single device and enable bidirectional communication with neural circuits with enhanced spatiotemporal precision. These technologies not only are facilitating a greater understanding of the brain, spinal cord and peripheral circuits in the context of health and disease, but also are informing the development of future closed-loop therapies for neurological, neuro-immune and neuroendocrine conditions.

The human nervous system is composed of a heterogeneous network of cells that communicate with one another through electrical, chemical and physical signals. Diseases of the nervous system, including Alzheimer's disease, Parkinson's disease and epilepsy, affect more than 100 million people and represent an annual burden greater than $800 billion in the United States alone[1]. Treatments for these disorders often rely on pharmacotherapy or implanted electrical stimulation devices, but they are generally not specific to neuronal subtypes and thus are accompanied by side effects. This lack of specificity arises as a result of a poor understanding of the underlying mechanisms of action of these interventions, alongside a lack of available tools to interact with the brain at meaningful levels of precision and depth. To fully appreciate this complexity, new probes must be developed to deliver and record signals through multiple modalities while minimizing unwanted side effects[2].

In this Review, we discuss principles that should be considered when designing next-generation neural interfaces to communicate bi-directionally with neural circuits through multiple modalities. Advances beyond classic electrical stimulation and recording techniques are likely to contribute to understanding and treating disorders of the nervous system. These efforts should help link the physiological processes associated with neuronal function to normal and pathological behavior and should also enable closed-loop bio-interfaces for therapeutic intervention.

Integration challenges in a multimodal neural interface

To understand neurological disorders and the mechanisms that drive behavior, neural circuits spanning areas across the brain must be interrogated (Fig. 1a). Moreover, each neuron has thousands of synaptic connections that are uniquely regulated by a palette of receptors that vary at the subcellular level (Fig. 1b–d). Neurotransmission also varies dramatically in temporal resolution, from the sub-microsecond span of action-potential firing to hour-long fluctuations in hormone concentrations or gene expression (Fig. 1e). Signaling events are heavily compounded, and their strength can vary by orders of magnitude; for example, neurotransmitter secretion occurs at concentrations ranging from picomolar (10^{-12} M) to micromolar (10^{-3} M) (ref. [3]).

Consequently, when designing neural interfaces, a multitude of factors must be considered, including spatial resolution, temporal precision, sensitivity and the cellular selectivity with which signals can be delivered or recorded. Neurotransmission is multimodal in nature; thus, the devices themselves should possess multiplexing capabilities, and the physical properties of the implanted hardware should be carefully engineered (Table 1). Size and flexibility must also be considered because the mechanical mismatch between stiff implanted devices (1–100 GPa) and the soft brain tissue (kilo- to megapascal) can yield tissue damage and elicit a foreign-body response that eventually blocks the interface through glial scarring. With these characteristics in mind, developments in materials, manufacturing techniques and signaling modalities should open doors to new experimental techniques and further understanding of neural processes.

Electrical recording and stimulation of neural activity

Since the first electroencephalography recording in 1938 (ref. [4]), numerous neural implants to stimulate and record electrical activity in the brain have been developed. Advanced fabrication techniques made available by the electronics industry have delivered silicon-based Utah arrays and Michigan probes[3,5] (Fig. 2a,b) and have enabled the extreme miniaturization and dense packing of electrodes in the Neuropixel[6]. Integrated with a complimentary metal-oxide-semiconductor (CMOS) platform, the Neuropixel offers 960 recording sites along 10-mm-long shanks with a 70 × 20 μm^2 cross-section and can record well-isolated action potentials from hundreds of neurons (Fig. 2c).

Because the mechanical and chemical mismatch between probes composed of hard materials (including metals, glasses and semiconductors) often yields a foreign-body response and gliosis in neighboring tissue[7,8], soft materials are increasingly being used in neural interfaces to minimize these effects. A notable example, the Neural Mesh, comprises 16 platinum recording or stimulating electrodes (20 μm and 150 μm in diameter, respectively) deposited onto gold interconnects sandwiched by layers of a photoresist SU-8 (20 μm wide and ~400 nm thick). The open architecture allows these probes to integrate with the brain tissue after injection via a needle[9] (Fig. 2d). The Neural Mesh permits recording of local field

[1]Research Laboratory of Electronics, Massachusetts Institute of Technology, Cambridge, MA, USA. [2]McGovern Institute for Brain Research, Massachusetts Institute of Technology, Cambridge, MA, USA. [3]Harvard/MIT Health Science & Technology Graduate Program, Cambridge, MA, USA. [4]Department of Material Science and Engineering, Massachusetts Institute of Technology, Cambridge, MA, USA. *e-mail: anikeeva@mit.edu

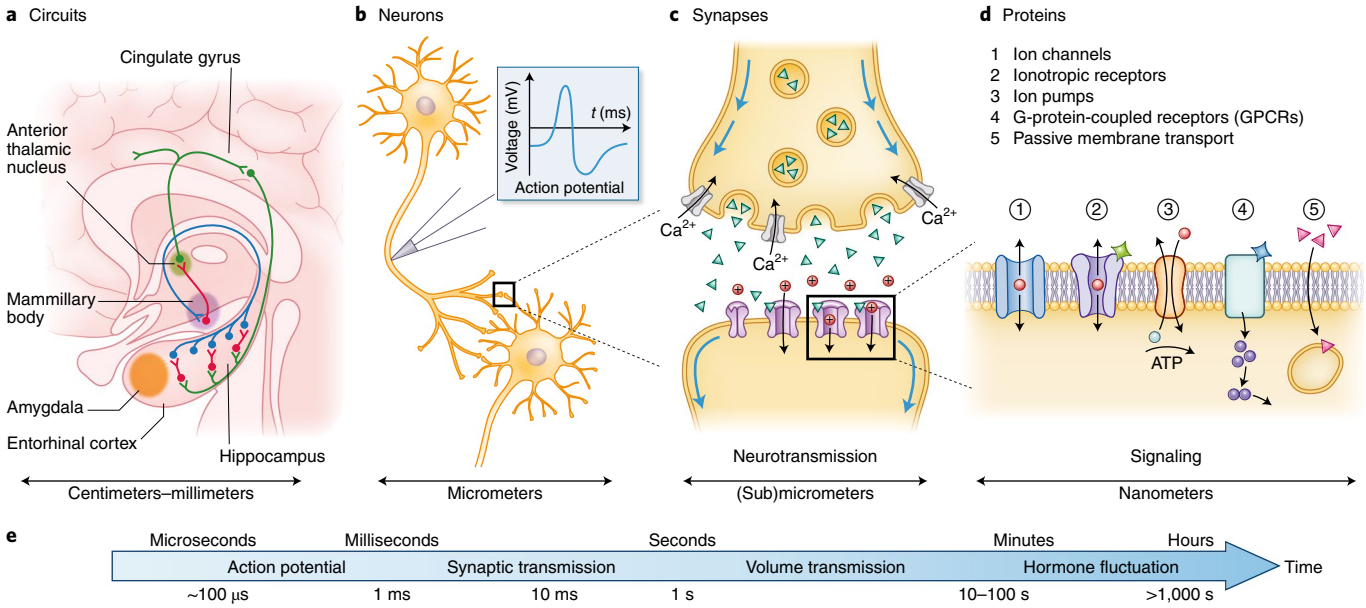

Fig. 1 | Overview of neuronal communication. A progressively zoomed-in view from a brain circuit to a neuron to a synapse to an ion channel. **a**, Example of a circuit spanning areas across the brain. The Papez circuit is involved in emotion and declarative memory. *t*, time. **b**, Neurons communicate via chemical and electrical signals. Action potential propagates to the synapse, where chemical neurotransmission takes place. **c**, The presynaptic neuron (top) releases neurotransmitters that diffuse in the synaptic cleft and bind receptor proteins on the postsynaptic cell (bottom). **d**, Diversity of membrane receptors in neurons involved in neurotransmission. **e**, Neuronal communication spans timescales ranging from sub-milliseconds to hours[137]. Credit: Debbie Maizels/Springer Nature

Table 1 | Comparison of electrical, optical, and chemical manipulation and recording of neuronal activity

Modality	Spatial resolution	Temporal resolution	Sensitivity	Selectivity
Electrical stimulation	Limited by current spreading and electrode dimensions	Sub-microsecond	Highly tunable	Limited; all cells surrounding probe experience field
Electrical recording	<10 µm	Sub-microsecond	>10 µV	Limited; pharmacology required to determine contributors to current
Optical stimulation	Single-cell optical stimulation[135]	Sub-microsecond	Highly tunable by irradiation power, wavelength, etc.	High; only light-sensitive reporters respond
Optical recording	Single cell[136]	Sub-microsecond; can record single action potentials	Limited by available reporters	High; selective biosensors for neurotransmitters and analytes have been developed
FSCV	>100 µm; limited by large devices required	≥100 ms	Can detect electroactive molecules over large concentration ranges	Moderate; care must be taken to validate electrochemical signatures of recording
Microdialysis	>150 µm; limited by large size of probes	Seconds to minutes	Sensitive toward a large range of analytes	High; defined by high-resolution chemical analytics[90]
Chemical stimulation	Limited by diffusion	Seconds to minutes; dictated by diffusion and metabolism	Moderate; tunable through dose applied	High; can be fine-tuned through synthetic chemistry
Chemical recording	Single cell[110]	Sub-microsecond[111]	Excellent; can be fine-tuned through synthetic chemistry	High; can be fine-tuned with synthetic chemistry

potentials and single-unit action potentials; it can deliver electrical stimulation over 8 months in the mouse brain. In a follow-up study, this platform was adapted to record single-unit activity from the retina in awake mice[10]. Mesh-based electrode arrays composed of porous and transparent graphene[11], or composite/metal nanowires[12] deposited on flexible and stretchable substrates, have been applied as conformal cortical surface probes and stimulation electrodes (Fig. 2e,f). These devices take the shape of the surface to which they are applied, and this approach has also been used to prepare spinal[13] and cardiac interfaces[14].

Organic conductors have been extensively explored in recording and stimulation electrodes, because of their promising mechanical and electrochemical interfaces with the neural tissue[15]. Because of its biochemical stability and ability to form both electronic and ionic interfaces with the cells in physiological fluids, the organic semiconductor poly(3,4-ethylenedioxythiophene):poly(styrene sulfonate) (PEDOT:PSS) and its chemical derivatives are often exploited in coatings to decrease the impedance and increase the charge-injection capacity (CIC) in miniaturized electrodes. For example, 8.4-µm carbon-fiber microelectrodes have been coated

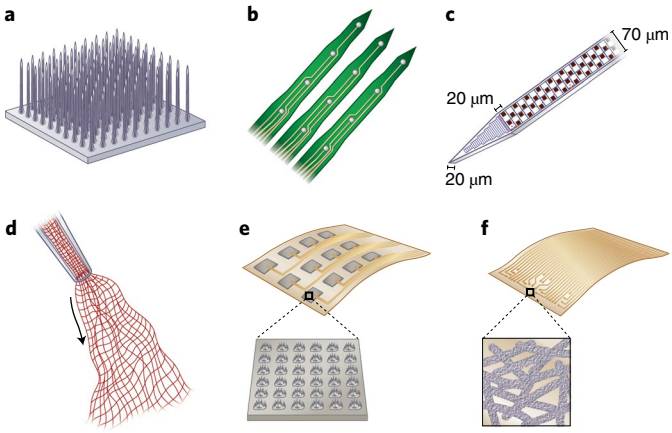

Fig. 2 | Probes for electrical stimulation and recording of neural activity. **a**,**b**, Microfabricated silicon-based Utah arrays[3] (**a**) and Michigan probes[5] (**b**). **c**, On the basis of the CMOS fabrication process, the Neuropixel features extreme miniaturization and dense packing of 960 recording electrodes[6]. **d**, Syringe-injectable mesh electronics based on gold, platinum and SU-8 integrate with the brain and record and stimulate neighboring neurons[9,10]. **e**,**f**, Examples of mesh-based electrode arrays: porous graphene electrode on SU-8 substrates[11] (**e**) and soft and stretchable electrode grids made of Au-TiO_2 nanowires embedded in PDMS[12] (**f**). Credit: Debbie Maizels/Springer Nature

with PEDOT:poly(toluenesulfonate) (PEDOT:PTS) to decrease the tip impedance from 6.8 MΩ to ~120 kΩ at 1 kHz (ref. [16]). This array is capable of recording single-unit action potentials from the rat motor cortex for 3 months, while inducing only negligible glial scarring[17]. Another system, the Neurogrid[18], uses PEDOT:PSS as a gate in organic electrochemical transistors on a 4-μm parylene C structure, thus permitting recording of isolated action potentials from the cortical surface with a high signal-to-noise ratio. A systematic study has recently quantified electronic and ionic transport between PEDOT-based electrodes and physiological environments, informing the design of interfaces for optimized signal-to-noise ratio and CIC[19].

The transition of high-resolution, low-modulus electrodes with improved impedance and CIC to the clinic will probably provide spatiotemporally precise alternatives to the millimeter-thick clinical deep-brain-stimulation electrodes. When paired with artifact-rejection circuits and algorithms to permit simultaneous stimulation and recording[20], these electrodes also empower closed-loop therapeutic neuromodulation. Furthermore, integration of electrophysiology and electrical stimulation with chemical and optical neural interrogation approaches should undoubtedly facilitate fundamental studies of neuronal dynamics and inform the abovementioned clinical interventions.

Light-controlled stimulation or silencing of neuronal activity with opsins

In the rapidly evolving field of optogenetics, cells or circuits can be genetically manipulated with sub-microsecond precision through incorporation of light-sensitive proteins[2,21]. The blue-light-sensitive cation channel channelrhodopsin 2 (ChR2), which depolarizes cells after activation, remains the workhorse tool for neural excitation[22], despite its early introduction to neuroscience (more than a decade ago; Fig. 3a). Thousands of studies have leveraged ChR2 to dissect the roles of specific brain regions, neuronal types, and projection circuits in controlling behaviors spanning motivation, movement, circadian rhythms, addiction, anxiety, memory, aggression and social interactions, among others[23–26]. Over the past decade, ChR variants with red-shifted activation spectra[27], modified kinetics[28] or subcellular localization[29] have also been developed to expand stimulation capabilities.

Complementary to neural excitation with photosensitive cation channels, inhibition is achieved with opsins that hyperpolarize the membrane. Inhibitory opsins, such as proton[30] or sodium[31] pumps, as well as chloride[32,33] channels, have been engineered for enhanced sensitivity and modified activation spectra and kinetics (Fig. 3b). For example, the blue-light-activated proton pump Arch3 silences neurotransmission by increasing cellular pH[30]. When fused to a pH-sensitive green fluorescent protein (GFP) and targeted to synaptic vesicles or lysosomes, the Arch-based pH probe pHeonix can control intracellular organelle acidification and provide an optical readout[34]. Moreover, rhodopsin-linked enzymes allow for optical control of the metabolism of second messengers, such as the rhodopsin–guanylyl cyclase CaRhGC and rhodopsin-adenylyl cyclase CaRhAC, which, after green irradiation, generate cyclic GMP or cyclic AMP, respectively[35] (Fig. 3c).

As the use of optogenetic tools in neuroscience continues to expand, so does the demand for probes capable of simultaneous optical modulation and monitoring of neural activity. Although commercially available silica fibers remain a staple of optogenetic studies, advanced probes, such as tapered optical fibers, allow for stimulation of multiple spatially restricted brain regions by using different wavelengths[36]. Moreover, the burgeoning interest from the neural engineering community has delivered a diversity of integrated optoelectronic probes, including Michigan-style[37] and Utah-style arrays[38], with monolithically integrated light-emitting devices (LEDs), microcontact printed flexible probes equipped with microscale LEDs (μLEDs)[39], arrays of transparent conductive nanopillars[40] and multifunctional polymer-based fibers[13,41,42]. These platforms have been extensively reviewed elsewhere[43], and in the later sections, we discuss these emerging tools with expanded capabilities that further empower optogenetic studies.

Light-controlled neural signaling using LOV domains and cryptochromes

Beyond opsins, other optogenetic motifs can be used to engineer light-responsive proteins to control enzymatic activity or gene expression through protein sequestration, rearrangement, fragment condensation or translocation[44]. The light oxygen voltage (LOV) domain can regulate activity or protein access through conformational rearrangements induced by blue-light irradiation. In the fast light- and activity-regulated expression (FLARE)[45] and Cal-Light approaches[46], a transcription factor is tethered to the membrane via a linker containing a calmodulin-binding motif and a protease-cleavage site that is sterically blocked by the dark-state LOV domain. During neuronal activation, an increased intracellular calcium ion concentration results in recruitment or reconstitution of a calmodulin-linked protease in proximity to the membrane linker. LOV-domain photoactivation unmasks the cleavage site, thereby releasing the transcription factor from the plasma membrane and driving gene expression (Fig. 3d). These optogenetic coincidence detectors can be applied to express opsins with activity-dependent cellular resolution, and specific neurons can later be activated or inhibited to confirm their role in behavior.

Optogenetic dimerizers (for example, the cryptochrome-based CRY2–CIB heterodimerization motif) can, after irradiation with blue light, fuse split enzymes or control protein translocation[47]. The CIB domain can be genetically targeted to specific subcellular locations, and fusion of CRY2 to a target protein can control localization on demand. This method has been used to generate an optogenetic cAMP-dependent protein kinase (optoPKA)[48], which can be reversibly activated on the mitochondria, cytoskeleton or plasma membrane (Fig. 3e). The emerging diversity of light-sensitive biological

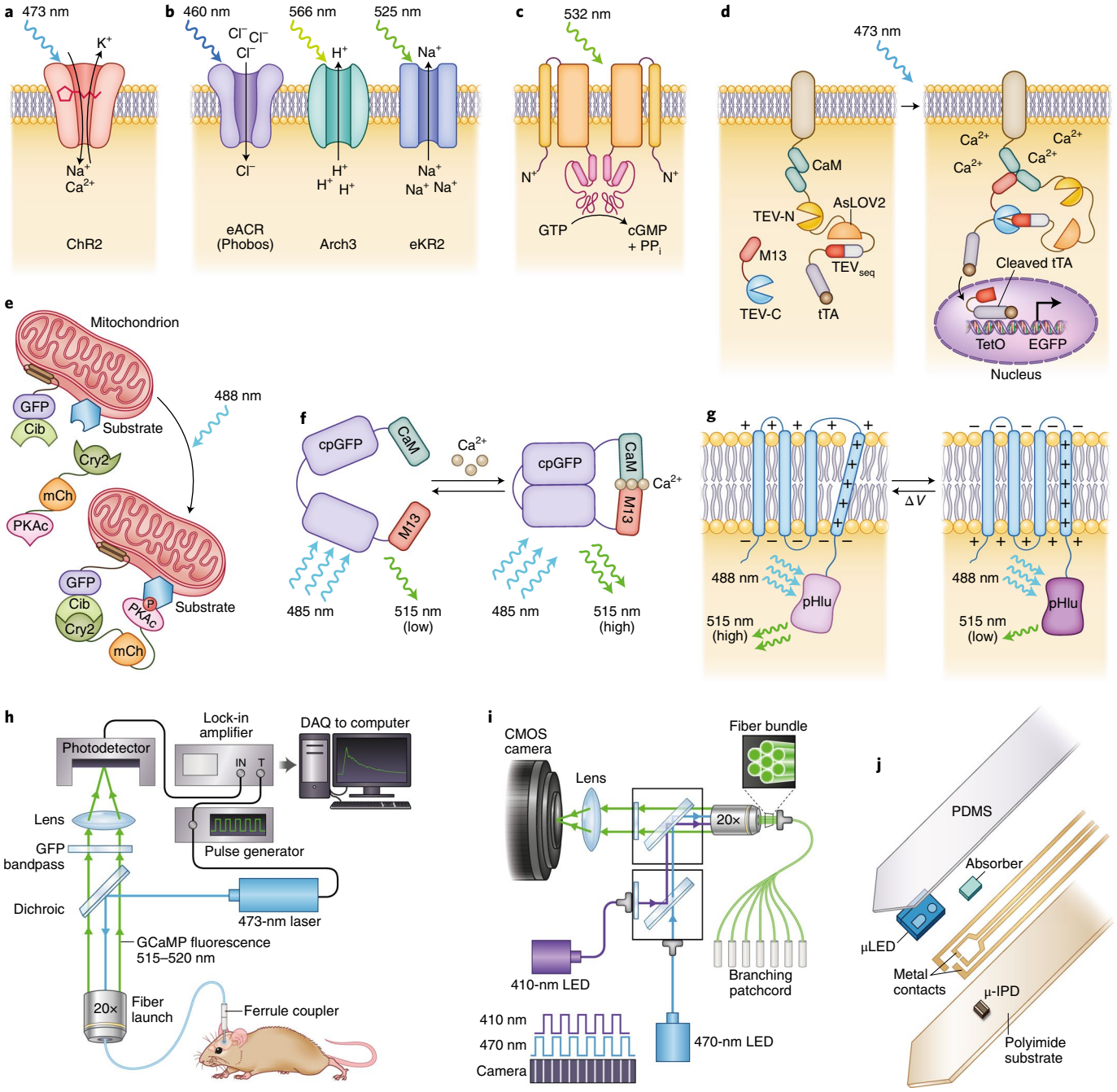

Fig. 3 | Optical neural stimulation and recording via genetic or non-genetic tools; sensitivity, orthogonality and requirements for hardware. **a**, ChR2 is a cation channel that mediates membrane depolarization after exposure to blue light. **b**, Recently developed inhibitory opsins, anion-conducting channelrhodopsin (eACR), proton-pump archaerhodopsin (Arch3) and enhanced sodium pump KR2 (eKR2). **c**, Rhodopsin-guanylyl cyclase chimeric protein CaRhGC consists of a photo-sensitive rhodopsin directly connected to the guanylyl cyclase via a coiled-coil stretch converts GTP to cGMP after green-light illumination[35]. **d**, In the Cal-Light approach, the increased Ca^{2+} in the cytosol M13 moiety binds the calmodulin Ca^{2+}-binding domain (CaM), thus restoring tobacco etch virus (TEV) protease function. *Avena sativa* phototropin 1 light-oxygen-voltage 2 (AsLOV2)-domain photoactivation unmasks TEV_{seq} cleavage site, which then releases cleaved tetracycline-controlled transcriptional activator (tTA) to translocate to the nucleus of the cell, where it initiates gene expression[46]. **e**, Light-triggered transfer of an optogenetic cAMP-dependent protein kinase (OptoPKA) from the cytoplasm to the mitochondria[48]. mCh is the mCherry fluorescent protein. **f**, GECI consists of Ca^{2+}-binding CaM, an M13 moiety and a circularly permuted green fluorescent protein (cpGFP). In GCaMP6, binding of Ca^{2+} induces the formation of CaM–M13 complex, which protects the fluorescent core and increases its quantum yield[138]. **g**, GEVI consists of a voltage-dependent domain and a fluorescent protein. Arclight consists of a voltage-sensing domain fused to a super ecliptic pHluorin (pHlu) reporter. Depolarization causes a conformational change resulting in a decrease in green fluorescence[138]. *V*, voltage. **h**,**i**, Single-fiber[65] (**h**) and multi-fiber (**i**) photometry[66]. Optical fibers transmit excitation light and collect light emitted from GECIs. DAQ, data acquisition. **j**, Micro-photometry system for deep-brain fluorescence recording integrating μLEDs and integrated photodetectors (IPDs) encapsulated by PDMS on a polyimide substrate[69]. Credit: Debbie Maizels/Springer Nature

machinery will enable the rational design of optogenetic tools to manipulate and probe molecular mechanisms of neurotransmission in vivo, with the goal of correlating these molecular processes to behavior in the context of health and disease.

Genetically encoded fluorescent reporters to monitor neural activity

Fluorescent reporters for ions or small molecules enable monitoring of neural activity from the subcellular to the population scales[49]. Genetically encoded calcium indicators (GECIs) remain the gold standard for imaging neural activity (Fig. 3f), and they enable entire cortical circuits to be monitored in awake head-fixed mice through wide-field and two-photon imaging[50]. In addition to green-emitting GCaMPs[51] (fusions of circularly permutated GFP, calmodulin and M13 peptide sequence from myosin light-chain kinase), red-shifted GECIs enable imaging in deeper tissues and can be used for multiplexed recording from orthogonal cell populations[52]. Similarly, genetically encoded voltage indicators (GEVIs) can record action potentials over large tissue volumes with sub-microsecond resolution. Closed-loop robotic directed evolution was used to engineer Archon1 for improved brightness and membrane localization[53]. In the 'Floxopatch' mouse line, the near-infrared opsin-based GEVI QuasAr2 (Fig. 3g) and the blue-shifted cation channel CheRiff are expressed in a Cre-dependent manner[54], thus enabling dual-color stimulation and recording in genetically defined cell populations. Other biomolecules or neurotransmitters can be imaged with encodable optical biosensors[55,56]. Probes for glutamate (SF-iGluSnFR)[57], dopamine (dLight1[58] and $GRAB_{DA}$[59]) acetylcholine (GACh)[60] or glycine (GlyFS)[61] enable real-time imaging of neurotransmitter release via one- or two-photon imaging. Expansion of this approach to other signaling molecules in combination with new probe hardware, sensors and multi-color imaging should permit dissection of the temporal dynamics of neurotransmitter and biomarker release, reuptake and ion flux.

Although conventional fluorescence microscopy enables recording of neural activity at multiple scales, it remains mostly limited to applications in head-fixed subjects. Implantable endoscopes based on gradient-index optics[62] and solid-state detectors (for example, Miniscope[63]) permit activity-dependent imaging in the brains of moving rodents. Although the former are available commercially, the latter can be assembled from off-the-shelf parts by using open-source instructions. Although fluorescence endoscopy of subcortical structures with the Miniscope requires removal of the cortical tissue, combining this method with two-photon excitation affords less invasive access to deeper brain areas[64].

Fiber photometry uses an implanted fiber optic to both excite and collect the emission from GECIs to record activity from populations of neurons[65] (Fig. 3h). Although spatial resolution is limited by the size of the fiber core and the scattering properties of the neural tissue, genetic targeting allows for monitoring of specified neurons in freely moving subjects. As many as seven spatially distinct brain regions can be simultaneously monitored in behaving animals through frame-projected independent-fiber photometry[66] (Fig. 3i), in which signals from a bundled fiber are integrated by a CMOS camera. When applied to GEVIs, the transmembrane electrical measurements performed optically (TEMPO) approach[67] can record local field potentials from defined cell populations without physiological noise fluctuations. The application of fiber photometry to other fluorescent biosensors should be instrumental in determining how neurotransmitters fluctuate in deep brain regions of behaving subjects. Notably, a multimode fiber-based endoscope permits the imaging of fluorescent proteins within deep brain regions[68]. Although it has yet to be applied to reporters of neural activity, this device may increase the applicability of fiber photometry to monitoring neural activity in deep brain regions with cellular resolution.

In addition to implantable optical probes that rely on external optoelectronics for signal detection, micro-contact printing techniques have recently permitted direct integration of μLEDs and photodetectors[69] (Fig. 3j). Such optoelectronic probes enable illumination and detection of reporter fluorescence at the point of implantation, thereby eliminating the need for collection optics and fiber tethers, and are compatible with wireless data and power transfer.

Electrical and microfluidic detection of neurotransmitters and biomarkers

Although signals propagate along the neuronal membrane in the form of electrical-potential waves, transmission between neurons occurs at the synaptic cleft via the release, reuptake and metabolism of neurotransmitters[70]. Understanding the spatiotemporal dynamics of chemical neurotransmission should enable dissection of the molecular mechanisms underlying many neurological disorders[71]. Electroactive biogenic amines, such as dopamine, norepinephrine, serotonin and histamine, can be detected in real time through in vivo fast-scan cyclic voltammetry (FSCV). This approach relies on rapid potential sweeps at implanted electrodes to oxidize and reduce nearby analyte molecules, and the voltammogram shape provides information about the target analyte[71,72] (Fig. 4a). FSCV excels in temporal resolution (<100 ms) and sensitivity, but it remains limited in terms of selectivity. Chemically similar electroactive species (for example, dopamine and norepinephrine) can complicate the analysis, but principal component analysis may be used to deconvolute signals from distinct neurotransmitters[73,74].

Despite decades of research, most FSCV experiments are still conducted with probes composed of a single carbon-fiber microelectrode housed in a glass capillary[75] (Fig. 4b). These probes have been used in long-term monitoring of dopamine dynamics in primates[76] and mice[77]. Moreover, simultaneous voltammetric detection of dopamine and oxygen can be combined with single-unit electrophysiological recordings to demonstrate fluctuations in these biomarkers correlated with widespread electrical activity after brain injury[78]. Notably, FSCV is compatible with optical stimulation of ChRs[79], and the development of more advanced probes with improved optical capabilities should allow FSCV to be used in conjunction with optical reporters to simultaneously monitor both electroactive and non-electroactive species with high temporal resolution.

Functional coatings can be deposited to improve electrode stability, sensitivity and analyte selectivity. Coating a tungsten electrode with a boron-doped diamond film has been found to improve the mechanical and electrochemical stability of FSCV probes[80]. Sensitivity is enhanced by increasing the electrochemical interface area and improving surface adsorption, as demonstrated with electrodeposited PEDOT-graphene oxide (PEDOT-GO) coatings[81]. PEDOT-GO, compared with uncoated carbon electrodes, increases dopamine detection sensitivity by 880% and decreases the limit of detection by 50% (to ~20 nM). Analyte selectivity can be enhanced by integrated size-exclusion membrane coatings for detection of low-molecular-weight molecules such as hydrogen peroxide[82]. Moreover, enzyme-coated electrodes widen the scope of accessible analytes; allow for detection of non-electroactive biomarkers, such as glucose[83,84]; and could be further expanded to detect lactate[85], choline and acetylcholine[86], and glutamate[87].

As a complement to voltammetry, microdialysis enables quantification of a vast array of biomarkers within the sampled fluid, independently of their electrochemical activity. Typical microdialysis probes consist of inlet and outlet capillaries within a hollow fiber that is sealed by a semi-permeable membrane and infused with buffer[88] (Fig. 4c). The collected analytes are subjected to chemical analytics including high-performance liquid chromatography and mass spectrometry[89], and sample derivatization permits detection of as many as 70 analyte molecules from a single sample[90]. Microdialysis

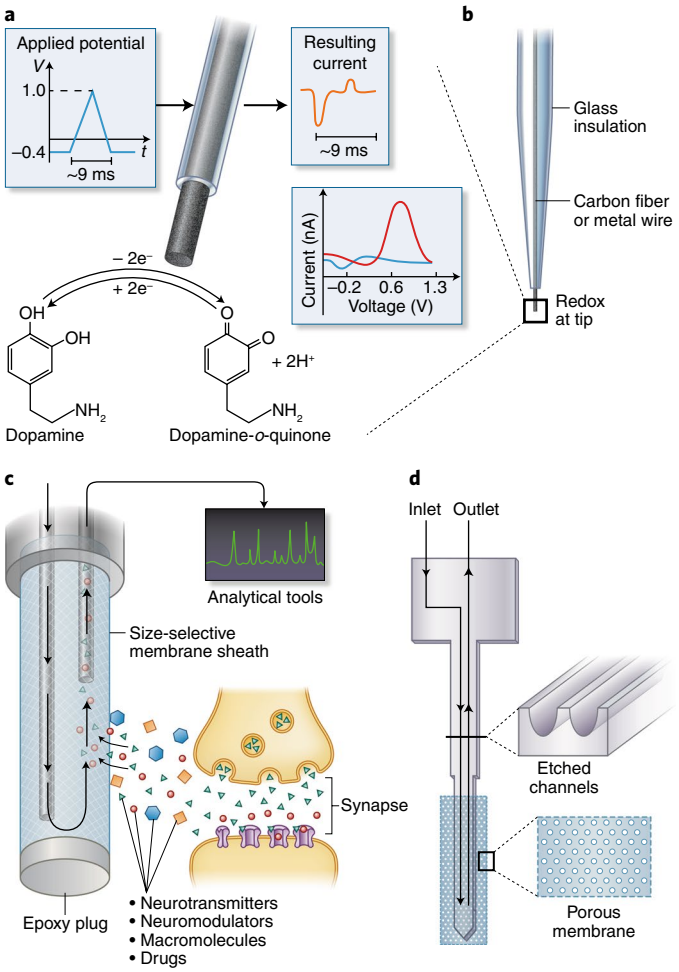

Fig. 4 | Chemical sensing with voltammetry and microdialysis. **a**, FSCV recording of dopamine concentration. After application of a triangle potential to the carbon-fiber microelectrode, dopamine oxidizes into dopamine-*o*-quinone and then is reduced back to dopamine. These electrochemical reactions contribute to the resulting current and form the basis of the cyclic voltammogram readout[71]. e^-, electron. **b**, Traditional FSCV probes are made of a carbon fiber or metal wire housed within borosilicate or fused-silica insulating sheaths. The redox reaction occurs at the exposed electrode tip[88]. **c**, A microdialysis probe is composed of inlet and outlet capillaries housed within a hollow-fiber shaft sealed by a size-selective membrane sheath infused with buffer. During microdialysis, chemical species diffuse into the hollow cavity and are collected for post hoc chemical analyses[88]. **d**, A microfabricated silicon-based microdialysis probe consists of a U-shaped microfluidic channel with a nanoporous membrane at the tip[94]. Credit: Debbie Maizels/Springer Nature

thus provides exquisite chemical resolution and a wide sensitivity range toward diverse analyte molecules[70]; however, the low sampling rate (often >10 min) and offline analysis limit its temporal resolution in real-time applications. The slow sampling rate also limits the spatial resolution, because diffusion of analytes through the tissue is a major factor at these timescales. Continuous online microdialysis (coMD)[91] is being used clinically for diagnosing and monitoring patients with traumatic brain injury[92]. The coMD approach uses ion-selective electrodes and dedicated sensors to perform real-time recording of multiple ions (including potassium) and small molecules (for example, glucose and lactate). It can also complement electrocorticography recordings to reveal how these biomarkers fluctuate with neural activity.

Microdialysis probes often exceed 200 μm in diameter[93]; thus, a microfabricated silicon-based probe with 45 × 180 μm² dimensions increases the spatial resolution and decreases the surrounding tissue damage[94] (Fig. 4d). This microfabricated silicon-based probe possesses an etched U-shaped channel and a nanoporous membrane along the tip and can quantify amphetamine-stimulated dopamine release in rat striatum with accuracy comparable to that of a standard dialysis probe. Similarly to FSCV, microdialysis is compatible with optical tools. A hybrid device composed of a light-guide embedded within a microdialysis probe has also been used to measure extracellular dopamine and glutamate in response to optogenetic stimulation within the mouse brain[95]. In a more recent example, an opto-dialysis probe has been used to monitor optically evoked release of multiple opioid peptides alongside dopamine, GABA (γ-aminobutyric acid) and glutamate in freely moving mice[96]. Future integration of more advanced microfluidic probes with optical capabilities should enable real-time imaging of neural activity concomitant with biomarker analysis with increased spatiotemporal precision.

Chemical approaches for stimulating neurons

Chemical probes can address the roles of specific receptors and downstream pathways in cell physiology. Designer receptors exclusively activated by designer drugs (DREADDs) are chemogenetic tools based on G-protein-coupled receptors (GPCRs) engineered to respond exclusively to an otherwise inert ligand[97,98]. DREADDs retain the natural downstream signaling properties of their parent receptors, thus allowing activation and inhibition of target neurons after systemic addition of the exogenous ligand. However, this approach offers limited spatial resolution and temporal precision restricted by slow on/off kinetics. For targeting endogenous receptors with increased precision, light-responsive molecules can transmit an optical stimulus into a cellular response. Caged ligands, whose activities are masked by a photo-labile protecting group, become irreversibly activated after illumination (Fig. 5a). Alternatively, permanent attachment of a photoswitch to a drug molecule can enable reversible optical control of the target[99], and a variety of ions/neurotransmitters and their receptors have therefore been placed under optical control[100]. Synthetic tuning of the photo-cages or switches permits activation or inactivation with far-red or two-photon irradiation[101,102] and can even target ligands to subcellular compartments[103,104].

Self-labeling enzyme tags covalently tether molecular probes to defined locations with subcellular accuracy[105]. These tags include SNAP (an O^6-alkylguanine DNA alkyltransferase that reacts with O^6-benzylguanine derivatives), CLIP (an O^2-alkylcytosine DNA alkyltransferase that reacts with O^2-benzylcytosine derivatives) or HaloTag (a haloalkane dehalogenase that reacts irreversibly with primary alkyl halides)—enzymes that react with a functional group at one end of the linker and thus tether the pharmacophore to the target. For example, the drugs acutely restricted by tethering (DART) approach uses the HaloTag to target an α-amino-3-hydroxy-5-methyl-4-isoxazolepropionic acid (AMPA)-receptor agonist to either striatal dopamine 1 (D1)- or D2-receptor-expressing cells in a Parkinson's disease mouse model[106]. Similarly, optical control of SNAP-metabotropic glutamate receptor 2 (mGluR2) receptors in retinal ganglion cells by using a photoswitchable glutamate tethered to BGAG (comprising a SNAP-reactive benzylguanine (BG) at one end, a linker and an azobenzene-glutamate (AG) at the other end) restores light responses in blind mouse retina in vivo, thereby enabling patterned vision[107] (Fig. 5b).

Importantly, multiplexed stimulation of distinct cell populations or receptor subtypes can be achieved through selective expression of orthogonal enzyme tags[108]. Antibodies can also be used to target molecules to defined locations. In the chromophore-assisted light inactivation (CALI) approach (Fig. 5c)[109], an antibody-conjugated

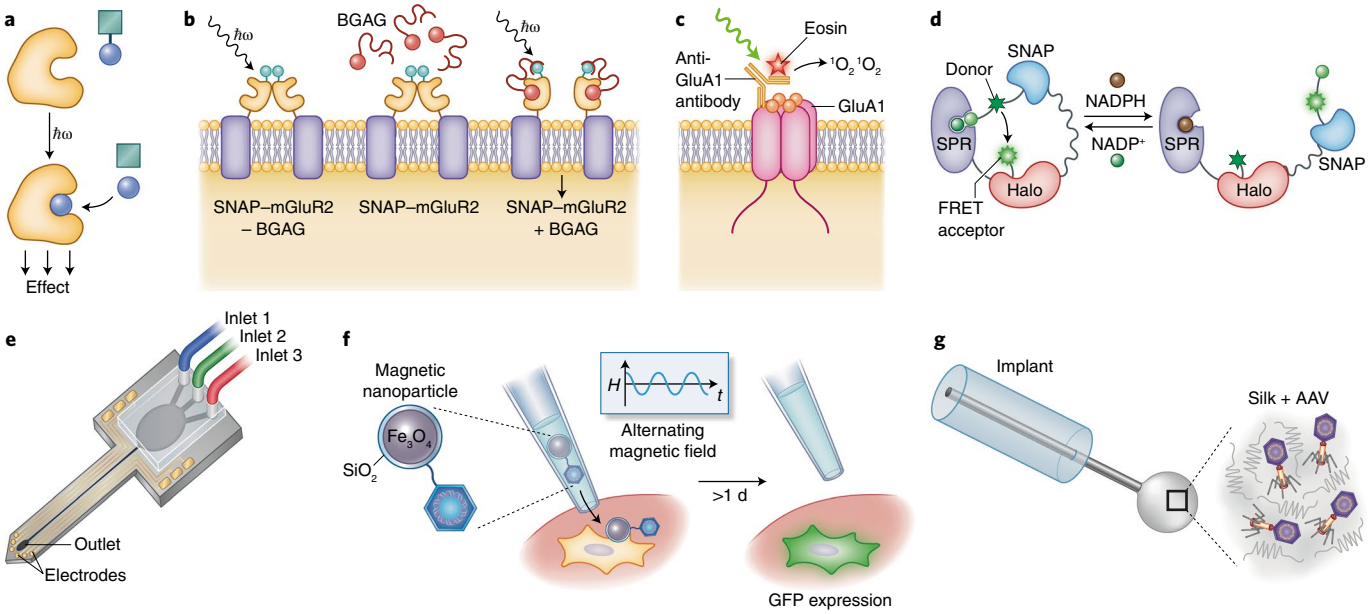

Fig. 5 | Technologies for chemical modulation and delivery. a, A protective group (the cage) is cleaved after illumination, and the ligand becomes biologically active[99]. **b**, An mGluR2 receptor modified to include a SNAP tag is optically controlled via a tethered photoswitchable glutamate BGAG[107]. **c**, Schematic representation of CALI. An anti-GluA1 monoclonal antibody is labeled with eosin, a photosensitizer. Photoactivation by green light and binding of the conjugated antibody to a GluA1 inactivates the targeted receptor containing GluA1 (ref. [109]). **d**, The semi-synthetic biosensor NADP-snifit measures NADPH/NADP+ levels via fluorescence shifts in a FRET pair tethered to a ligand-binding domain by HaloTags and SNAP tags[113]. SPR, sepiapterin reductase. **e**, Schematic representation of the Chemtrode, a microfabricated probe integrating a microelectrode array with a microfluidic channel connected to three separate inlets[114]. **f**, A GFP-gene-carrying virus is reversibly bound to a magnetic nanoparticle that is brought into physical contact with the target cell by using magnetic forces and then released after application of an alternating magnetic field[116]. *H*, magnetic field strength. **g**, Coating of silk fibroin mixed with AAV capsids for widespread virus expression in the vicinity of the device[117]. Credit: Debbie Maizels/Springer Nature

photosensitizer can selectively inactivate target receptors through localized generation of singlet oxygen. This method has been used to inactivate AMPA receptors in the mouse hippocampus and to erase fear memory in vivo during behavior. Future synthetic efforts should expand these approaches to other ligands and receptors, and implantable devices that permit simultaneous viral and chemical delivery alongside optical stimulation should facilitate the use of these technologies in freely moving animals.

Synthetic and semi-synthetic probes for molecule and ion detection

Small-molecule ion- or voltage-sensitive dyes enable imaging of neural activity without the need for genetic manipulation, and their selectivity and sensitivity can be systematically tuned through chemical modification. For example, the red-shifted calcium sensor Cal-590 permits in vivo two-photon imaging up to 1 mm deep within the mouse cortex[110]. It can be applied by extracellular perfusion or localized to single cells by electroporation through a patch pipette. Rhodamine-based voltage dyes possess increased dynamic range, permit visualization of single action potentials in deep tissues[111] and can be used in conjunction with green-emitting calcium indicators for multiplexed imaging.

Semi-synthetic biosensors have the advantage of genetic targetability while retaining the synthetic malleability of small-molecule dyes. Tethering hydrogen-sensitive dyes to the insides of synaptic vesicles by using SNAP tags allows for visualization of exocytosis and endocytosis in hippocampal neurons[112]. An alternative strategy for measuring NAD^+ or NADPH/$NADP^+$ levels (NAD-Snifit and NADP-Snifit, respectively) uses orthogonal bioconjugation (SNAP tags and HaloTags) to tether a Förster resonance energy transfer (FRET) fluorophore pair to defined locations on a ligand-binding domain[113]. FRET changes induced by analyte binding allow NAD(P) levels to be quantified in real time (Fig. 5d). These hybrid probes can be applied to a wide array of analyte molecules and used in vivo alongside the development of the appropriate hardware.

Approaches for small-molecule and gene delivery

Achieving the delivery of small molecules in vivo with precision comparable to that of chemical neurotransmission remains a challenge. Local injections bypass the blood–brain barrier and generate high local drug concentrations while decreasing the potential for off-target effects associated with systemic injections. Although conventional cannulas are still commonly used, microfabricated probes with enhanced capabilities and improved biocompatibility have emerged. For instance, the Chemtrode integrates a microfluidic channel with a microelectrode array, thereby enabling injection of as many as three different drugs alongside simultaneous electrophysiology at seven recording sites[114] (Fig. 5e). The microfluidic ion pump μFIP uses electrophoresis to drive solvent-free delivery of ions, such as K^+ and $GABA^-$, across a membrane to the target region[115].

Controlling gene delivery across different scales is vital to understanding the roles of individual cells or to interface with large functional areas of the brain (Fig. 5f). Single-cell transduction can be achieved through the virus-stamping approach[116], in which viral particles are reversibly bound to the surfaces of iron nanoparticles placed in a micropipette solution. The micropipette is inserted into the brain and positioned against the target cell, and magnetic-field application directs the particles to the target-cell surface. This technique is compatible with several viruses commonly used in optogenetics and can be exploited to transduce other biosensors into single cells. In addition, large functional areas can be transduced by functional coatings of silk fibroin mixed with adeno-associated virus (AAV) capsids (Fig. 5g). When applied to the surfaces of implants,

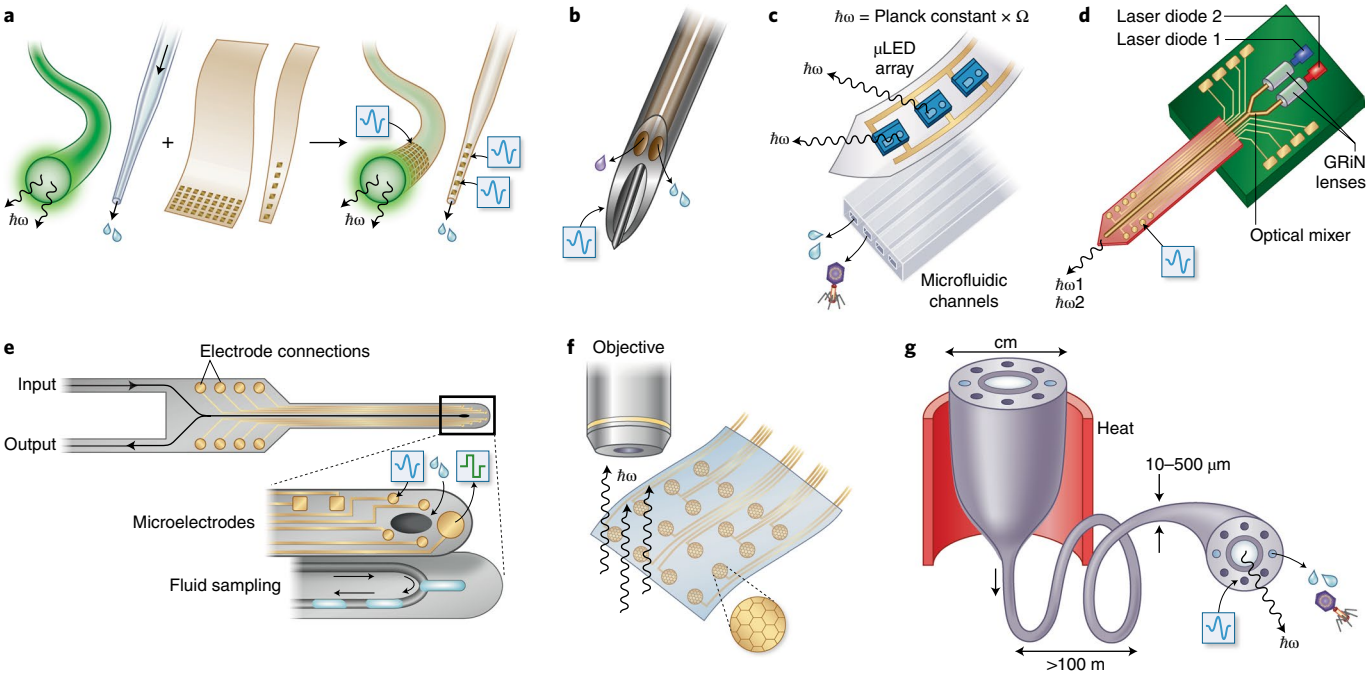

Fig. 6 | Multimodal integration. a, Adhesion of a nanoelectronic coating onto an optical fiber or a micropipette results in bi-modal probes[119]. **b**, The MiNDS consists of two borosilicate microfluidic channels and a tungsten recording electrode inserted into a stainless-steel needle[120]. **c**, Bonding of an μ-iLED array on a polymer substrate to a soft PDMS microfluidic device leads to a flexible optofluidic probe[39]. **d**, The dual-color optoelectrode fuses monolithically integrate an optical mixer with a Michigan-style probe[122]. **e**, A bi-modal neural probe monolithically integrates microfluidic channels with recording and stimulation electrodes[124]. **f**, Transparent graphene electrodes fabricated on a flexible parylene C substrate permit electrophysiological recording concomitant with optical imaging with GEVI and optical coherence tomography[126]. **g**, Thermal drawing of multi-material macroscale models, preforms, into kilometers of fibers comprising polymer waveguides, conductive composite or metallic electrodes, and microfluidic channels[13,41,42]. Credit: Debbie Maizels/Springer Nature

such as optical fibers or cranial windows[117], this approach ensures widespread virus expression at the site of the implant and simplifies the surgical implantation procedure. Alternatively, engineered viral capsids that can cross the blood–brain barrier, such as AAV-PHP.eB, enable widespread non-invasive labeling throughout the entire central nervous system after systemic injection[118]. These approaches should be especially useful when applied to optogenetic probes or biosensors for expression in large mammals.

Multi-modal interaction with cells and tissues

To keep pace with the ever-expanding palette of molecular and genetic tools for controlling and recording neural activity, emerging neural interfaces must integrate multiple functional features to deliver electrical, optical and chemical signals to and from neural tissue. Such probes should enable bi-directional communication with neural circuits and accelerate fundamental studies of their physiological and pathological outputs.

The most straightforward approach to integrate multiple functionalities is to fuse disparate existing technologies. For example, addition of a nanoelectronic coating to the surface of a device (such as a silica optical fiber or a micropipette) endows it with electrical recording capabilities for delivering a bi-modal probe[119] (Fig. 6a). Alternatively, a miniaturized neural drug delivery system (MiNDS) has been reported, which relies on a tungsten recording electrode and two microfluidic channels housed in a stainless-steel needle[120] (Fig. 6b). This device has been used to record and chemically stimulate deep brain regions in non-human primates. The fusion of soft microfluidic channels to an integrated array of inorganic μ-LEDs (μ-iLEDs) on a flexible substrate has also been used to create an optofluidic system that not only delivers drugs and viruses to the brains of freely moving rodents but also concurrently confers the ability to photostimulate neural activity[39] (Fig. 6c). Although this approach enables the design of multifunctional devices, it is often limited by the device footprint, which increases with the addition of each new functionality.

Leveraging well-established micro- and nano-fabrication techniques permits scalable production of miniaturized devices with densely packed features. For example, optoelectronic integration has been applied to produce a multi-shank optoelectrode enabling dual-color photostimulation and electrical recording at multiple sites[121,122] (Fig. 6d). Each silicon shank integrates two laser diodes and iridium electrodes, thus allowing recording alongside dual-color photostimulation in vivo. Similarly, using polydimethylsiloxane (PDMS) as a substrate, the electronic dura matter integrates microfluidic channels with recording and stimulating electrodes onto a flexible, transparent and stretchable probe, which has been used to restore locomotion after spinal-cord injury in rodents[123]. Microfabrication techniques have also been used to prepare a T-junction low-flow, push–pull microdialysis probe, which additionally houses platinum electrodes capable of electrical stimulation and recording[124] (Fig. 6e).

The use of transparent substrates and electrodes can endow electrophysiological probes with optical capabilities without increasing their footprint. The deposition of transparent electrode arrays onto polymer substrates permits simultaneous electrical recording and optogenetic stimulation[125] or fluorescent imaging with GECI[126] on the cortical surface (Fig. 6f). Two-photon imaging and optogenetic excitation extend these approaches to deeper tissues[127,128]. In another approach, silicon-based biointerfaces leverage the photoelectric, photoacoustic and photothermal properties of silicon to stimulate neurons through multiple modalities. These biointerfaces can be shaped into nanowires, flat nanomembranes or flexible mesh

arrays to generate thermal, faradaic or mechanical signals after irradiation[129]. These interfaces can also be tailored to allow for intercellular, intracellular and extracellular optical control of neural activity without the need for genetic modification.

An alternative strategy to enable multifunctional integration at the microscale, used by our laboratory, is to apply thermal drawing of multi-material fibers offers[42] (Fig. 6g). Fibers combining optical neuromodulation, microfluidic delivery of drugs and viruses, and electrophysiological recording capabilities can be produced in kilometer lengths from macroscale models through application of heat and tension. These devices have recently enabled monitoring of opsin expression in cell bodies and axonal terminals, thus informing projection mapping in behavioral studies[41,130]. Moreover, application of fiber drawing to elastomers has delivered stretchable probes suitable for chronic recording and optogenetic neuromodulation in the rodent spinal cord[13]. In the future, innovations in materials chemistry and thermal drawing techniques are anticipated to expand the sensing and modulation capabilities of fiber probes while maintaining their miniature and flexible form factors[131–133].

Conclusions and perspective

The nervous system is formed by a vast network of cells communicating through a plethora of stimuli. To fully appreciate this complexity, next-generation technologies must communicate with the neural tissue bi-directionally through a variety of modalities, time-scales and sensitivities, while spanning the nanometer to centimeter scales. Fabrication techniques and materials must evolve accordingly to accommodate novel optical and chemical probes to facilitate their use in behaving subjects, while enabling continuous recording of multiple biomarkers. Importantly, alongside this ever-expanding toolkit of neural probes comes increasing experimental complexity that may impede data interpretation. Certain modalities are not compatible when applied simultaneously in spatially restricted areas of the brain and can cause confounding artifacts that skew experimental observations. Therefore, great care must be taken when selecting tools for each experiment, and appropriate control experiments must be performed to avoid unsupported or erroneous conclusions. However, when used correctly, these tools should enable studies of the molecular mechanisms underlying behavioral and physiological phenotypes and facilitate integration of molecular and systems neuroscience. The insights delivered by such integrated studies should inform therapeutic approaches for neurological and psychiatric conditions with heterogeneous pathophysiology and temporally evolving signatures.

Although most tool development to date has focused on interrogation of neurons, glia are emerging as increasingly important players in functioning nervous system, and approaches to exclusively target glial biology and signaling are urgently needed. Applications to other electroactive tissues present entirely different challenges, such as cell-type diversity, different time-scales for activation, and different sets of chemical and physical signals[134]. These extensive applications provide biologists and engineers with endless research opportunities, and the urgency to develop therapeutic interventions for disorders of the aging nervous system should motivate the translation of these emergent approaches and insights from the lab into the clinic.

Received: 13 September 2018; Accepted: 26 June 2019;
Published online: 12 August 2019

References

1. Gooch, C. L., Pracht, E. & Borenstein, A. R. The burden of neurological disease in the United States: a summary report and call to action. *Ann. Neurol.* **81**, 479–484 (2017).
2. Rajasethupathy, P., Ferenczi, E. & Deisseroth, K. Targeting neural circuits. *Cell* **165**, 524–534 (2016).
3. Nordhausen, C. T., Maynard, E. M. & Normann, R. A. Single unit recording capabilities of a 100 microelectrode array. *Brain Res.* **726**, 129–140 (1996).
4. Berger, H. Uber das Elektrenkephalogramm des Menschen. IV. *Nov. Acta Leopoldina* **6**, 174–309 (1938).
5. Campbell, P. K., Jones, K. E., Huber, R. J., Horch, K. W. & Normann, R. A. A silicon-based, three-dimensional neural interface: manufacturing processes for an intracortical electrode array. *IEEE Trans. Biomed. Eng.* **38**, 758–768 (1991).
6. Jun, J. J. et al. Fully integrated silicon probes for high-density recording of neural activity. *Nature* **551**, 232–236 (2017).
7. Ward, M. P., Rajdev, P., Ellison, C. & Irazoqui, P. P. Toward a comparison of microelectrodes for acute and chronic recordings. *Brain Res.* **1282**, 183–200 (2009).
8. Nolta, N. F., Christensen, M. B., Crane, P. D., Skousen, J. L. & Tresco, P. A. BBB leakage, astrogliosis, and tissue loss correlate with silicon microelectrode array recording performance. *Biomaterials* **53**, 753–762 (2015).
9. Fu, T. M. et al. Stable long-term chronic brain mapping at the single-neuron level. *Nat. Methods* **13**, 875–882 (2016).
10. Hong, G. et al. A method for single-neuron chronic recording from the retina in awake mice. *Science* **360**, 1447–1451 (2018).
11. Lu, Y., Lyu, H., Richardson, A. G., Lucas, T. H. & Kuzum, D. Flexible neural electrode array based-on porous graphene for cortical microstimulation and sensing. *Sci. Rep.* **6**, 33526 (2016).
12. Tybrandt, K. et al. High-density stretchable electrode grids for chronic neural recording. *Adv. Mater.* **30**, e1706520 (2018).
13. Lu, C. et al. Flexible and stretchable nanowire-coated fibers for optoelectronic probing of spinal cord circuits. *Sci. Adv.* **3**, e1600955 (2017).
14. Choi, S. et al. Highly conductive, stretchable and biocompatible Ag-Au core-sheath nanowire composite for wearable and implantable bioelectronics. *Nat Nanotechnol.* **13**, 1048–1056 (2018).
15. Inal, S., Rivnay, J., Suiu, A.-O., Malliaras, G. G. & McCulloch, I. Conjugated polymers in bioelectronics. *Acc. Chem. Res.* **51**, 1368–1376 (2018).
16. Patel, P. R. et al. Insertion of linear 8.4 µm diameter 16 channel carbon fiber electrode arrays for single unit recordings. *J. Neural Eng.* **12**, 046009 (2015).
17. Patel, P. R. et al. Chronic in vivo stability assessment of carbon fiber microelectrode arrays. *J. Neural Eng.* **13**, 066002 (2016).
18. Khodagholy, D. et al. NeuroGrid: recording action potentials from the surface of the brain. *Nat. Neurosci.* **18**, 310–315 (2015).
19. Rivnay, J. et al. Structural control of mixed ionic and electronic transport in conducting polymers. *Nat. Commun.* **7**, 11287 (2016).
20. Zhou, A., Johnson, B. C. & Muller, R. Toward true closed-loop neuromodulation: artifact-free recording during stimulation. *Curr. Opin. Neurobiol.* **50**, 119–127 (2018).
21. Zemelman, B. V., Lee, G. A., Ng, M. & Miesenböck, G. Selective photostimulation of genetically chARGed neurons. *Neuron* **33**, 15–22 (2002).
22. Deisseroth, K. & Hegemann, P. The form and function of channelrhodopsin. *Science* **357**, eaan5544 (2017).
23. Liu, X. et al. Optogenetic stimulation of a hippocampal engram activates fear memory recall. *Nature* **484**, 381–385 (2012).
24. Felix-Ortiz, A. C., Burgos-Robles, A., Bhagat, N. D., Leppla, C. A. & Tye, K. M. Bidirectional modulation of anxiety-related and social behaviors by amygdala projections to the medial prefrontal cortex. *Neuroscience* **321**, 197–209 (2016).
25. Adamantidis, A. R., Zhang, F., Aravanis, A. M., Deisseroth, K. & de Lecea, L. Neural substrates of awakening probed with optogenetic control of hypocretin neurons. *Nature* **450**, 420–424 (2007).
26. Gradinaru, V., Mogri, M., Thompson, K. R., Henderson, J. M. & Deisseroth, K. Optical deconstruction of parkinsonian neural circuitry. *Science* **324**, 354–359 (2009).
27. Mager, T. et al. High frequency neural spiking and auditory signaling by ultrafast red-shifted optogenetics. *Nat. Commun.* **9**, 1750 (2018).
28. Ronzitti, E. et al. Sub-millisecond optogenetic control of neuronal firing with two-photon holographic photoactivation of Chronos. *J. Neurosci.* **37**, 10679–10689 (2017).
29. Tkatch, T. et al. Optogenetic control of mitochondrial metabolism and Ca^{2+} signaling by mitochondria-targeted opsins. *Proc. Natl Acad. Sci. USA* **114**, E5167–E5176 (2017).
30. El-Gaby, M. et al. Archaerhodopsin selectively and reversibly silences synaptic transmission through altered pH. *Cell Rep.* **16**, 2259–2268 (2016).
31. Grimm, C., Silapetere, A., Vogt, A., Bernal Sierra, Y. A. & Hegemann, P. Electrical properties, substrate specificity and optogenetic potential of the engineered light-driven sodium pump eKR2. *Sci. Rep.* **8**, 9316 (2018).
32. Wietek, J. et al. Anion-conducting channelrhodopsins with tuned spectra and modified kinetics engineered for optogenetic manipulation of behavior. *Sci. Rep.* **7**, 14957 (2017).

33. Chuong, A. S. et al. Noninvasive optical inhibition with a red-shifted microbial rhodopsin. *Nat. Neurosci.* **17**, 1123–1129 (2014).
34. Rost, B. R. et al. Optogenetic acidification of synaptic vesicles and lysosomes. *Nat. Neurosci.* **18**, 1845–1852 (2015).
35. Scheib, U. et al. Rhodopsin-cyclases for photocontrol of cGMP/cAMP and 2.3 Å structure of the adenylyl cyclase domain. *Nat. Commun.* **9**, 2046 (2018).
36. Pisanello, F. et al. Dynamic illumination of spatially restricted or large brain volumes via a single tapered optical fiber. *Nat. Neurosci.* **20**, 1180–1188 (2017).
37. Wu, F. et al. Monolithically Integrated μLEDs on silicon neural probes for high-resolution optogenetic studies in behaving animals. *Neuron* **88**, 1136–1148 (2015).
38. Wang, J. et al. Integrated device for combined optical neuromodulation and electrical recording for chronic in vivo applications. *J. Neural Eng.* **9**, 016001 (2012).
39. Jeong, J. W. et al. Wireless optofluidic systems for programmable in vivo pharmacology and optogenetics. *Cell* **162**, 662–674 (2015).
40. Lee, J., Ozden, I., Song, Y.-K. & Nurmikko, A. V. Transparent intracortical microprobe array for simultaneous spatiotemporal optical stimulation and multichannel electrical recording. *Nat. Methods* **12**, 1157–1162 (2015).
41. Park, S. et al. One-step optogenetics with multifunctional flexible polymer fibers. *Nat. Neurosci.* **20**, 612–619 (2017).
42. Canales, A. et al. Multifunctional fibers for simultaneous optical, electrical and chemical interrogation of neural circuits in vivo. *Nat. Biotechnol.* **33**, 277–284 (2015).
43. Chen, R., Canales, A. & Anikeeva, P. Neural recording and modulation technologies. *Nat. Rev. Mater.* **2**, 16093 (2017).
44. Rost, B. R., Schneider-Warme, F., Schmitz, D. & Hegemann, P. Optogenetic tools for subcellular applications in neuroscience. *Neuron* **96**, 572–603 (2017).
45. Wang, W. et al. A light- and calcium-gated transcription factor for imaging and manipulating activated neurons. *Nat. Biotechnol.* **35**, 864–871 (2017).
46. Lee, D., Hyun, J. H., Jung, K., Hannan, P. & Kwon, H. B. A calcium- and light-gated switch to induce gene expression in activated neurons. *Nat. Biotechnol.* **35**, 858–863 (2017).
47. Taslimi, A. et al. Optimized second-generation CRY2–CIB dimerizers and photoactivatable Cre recombinase. *Nat. Chem. Biol.* **12**, 425–430 (2016).
48. O'Banion, C. P. et al. Design and profiling of a subcellular targeted optogenetic cAMP-dependent protein kinase. Cell. *Chem. Biol.* **25**, 100–109.e8 (2018).
49. Kim, E. H., Chin, G., Rong, G., Poskanzer, K. E. & Clark, H. A. Optical probes for neurobiological sensing and imaging. *Acc. Chem. Res.* **51**, 1023–1032 (2018).
50. Allen, W. E. et al. Global representations of goal-directed behavior in distinct cell types of mouse neocortex. *Neuron* **94**, 891–907.e6 (2017).
51. Ohkura, M. et al. Genetically encoded green fluorescent Ca^{2+} indicators with improved detectability for neuronal Ca^{2+} signals. *PLoS One* **7**, e51286 (2012).
52. Dana, H. et al. Sensitive red protein calcium indicators for imaging neural activity. *eLife* **5**, e12727 (2016).
53. Piatkevich, K. D. et al. A robotic multidimensional directed evolution approach applied to fluorescent voltage reporters. *Nat. Chem. Biol.* **14**, 352–360 (2018).
54. Lou, S. et al. Genetically targeted all-optical electrophysiology with a transgenic Cre-dependent optopatch mouse. *J. Neurosci.* **36**, 11059–11073 (2016).
55. Bolbat, A. & Schultz, C. Recent developments of genetically encoded optical sensors for cell biology. *Biol. Cell* **109**, 1–23 (2017).
56. Lin, M. Z. & Schnitzer, M. J. Genetically encoded indicators of neuronal activity. *Nat. Neurosci.* **19**, 1142–1153 (2016).
57. Marvin, J. S. et al. Stability, affinity and chromatic variants of the glutamate sensor iGluSnFR. *Nat. Methods* **15**, 936–939 (2018).
58. Patriarchi, T. et al. Ultrafast neuronal imaging of dopamine dynamics with designed genetically encoded sensors. *Science* **360**, eaat4422 (2018).
59. Sun, F. et al. A genetically encoded fluorescent sensor enables rapid and specific detection of dopamine in flies, fish, and mice. *Cell* **174**, 481–496.e19 (2018).
60. Jing, M. et al. A genetically encoded fluorescent acetylcholine indicator for in vitro and in vivo studies. *Nat. Biotechnol.* **36**, 726–737 (2018).
61. Zhang, W. H. et al. Monitoring hippocampal glycine with the computationally designed optical sensor GlyFS. *Nat. Chem. Biol.* **14**, 861–869 (2018).
62. Flusberg, B. A. et al. High-speed, miniaturized fluorescence microscopy in freely moving mice. *Nat. Methods* **5**, 935–938 (2008).
63. Ghosh, K. K. et al. Miniaturized integration of a fluorescence microscope. *Nat. Methods* **8**, 871–878 (2011).
64. Zong, W. et al. Fast high-resolution miniature two-photon microscopy for brain imaging in freely behaving mice. *Nat. Methods* **14**, 713–719 (2017).
65. Gunaydin, L. A. et al. Natural neural projection dynamics underlying social behavior. *Cell* **157**, 1535–1551 (2014).
66. Kim, C. K. et al. Simultaneous fast measurement of circuit dynamics at multiple sites across the mammalian brain. *Nat. Methods* **13**, 325–328 (2016).
67. Marshall, J. D. et al. Cell-type-specific optical recording of membrane voltage dynamics in freely moving mice. *Cell* **167**, 1650–1662.e15 (2016).
68. Turtaev, S. et al. High-fidelity multimode fibre-based endoscopy for deep brain in vivo imaging. *Light Sci. Appl.* **7**, 92 (2018).
69. Lu, L. et al. Wireless optoelectronic photometers for monitoring neuronal dynamics in the deep brain. *Proc. Natl Acad. Sci. USA* **115**, E1374–E1383 (2018).
70. Anderzhanova, E. & Wotjak, C. T. Brain microdialysis and its applications in experimental neurochemistry. *Cell Tissue Res.* **354**, 27–39 (2013).
71. Robinson, D. L., Hermans, A., Seipel, A. T. & Wightman, R. M. Monitoring rapid chemical communication in the brain. *Chem. Rev.* **108**, 2554–2584 (2008).
72. Roberts, J. G. & Sombers, L. A. Fast-scan cyclic voltammetry: chemical sensing in the brain and beyond. *Anal. Chem.* **90**, 490–504 (2018).
73. Rodeberg, N. T. et al. Construction of training sets for valid calibration of in vivo cyclic voltammetric data by principal component analysis. *Anal. Chem.* **87**, 11484–11491 (2015).
74. Johnson, J. A., Rodeberg, N. T. & Wightman, R. M. Failure of standard training sets in the analysis of fast-scan cyclic voltammetry data. *ACS Chem. Neurosci.* **7**, 349–359 (2016).
75. Rodeberg, N. T., Sandberg, S. G., Johnson, J. A., Phillips, P. E. M. & Wightman, R. M. Hitchhiker's Guide to Voltammetry: acute and chronic electrodes for in vivo fast-scan cyclic voltammetry. *ACS Chem. Neurosci.* **8**, 221–234 (2017).
76. Schwerdt, H. N. et al. Long-term dopamine neurochemical monitoring in primates. *Proc. Natl Acad. Sci. USA* **114**, 13260–13265 (2017).
77. Clark, J. J. et al. Chronic microsensors for longitudinal, subsecond dopamine detection in behaving animals. *Nat. Methods* **7**, 126–129 (2010).
78. Hobbs, C. N., Johnson, J. A., Verber, M. D. & Mark Wightman, R. An implantable multimodal sensor for oxygen, neurotransmitters, and electrophysiology during spreading depolarization in the deep brain. *Analyst* **142**, 2912–2920 (2017).
79. Hamid, A. A. et al. Mesolimbic dopamine signals the value of work. *Nat. Neurosci.* **19**, 117–126 (2016).
80. Bennet, K. E. et al. A diamond-based electrode for detection of neurochemicals in the human brain. *Front. Hum. Neurosci.* **10**, 102 (2016).
81. Taylor, I. M. et al. Enhanced dopamine detection sensitivity by PEDOT/graphene oxide coating on in vivo carbon fiber electrodes. *Biosens. Bioelectron.* **89**, 400–410 (2017).
82. Wilson, L. R., Panda, S., Schmidt, A. C. & Sombers, L. A. Selective and mechanically robust sensors for electrochemical measurements of real-time hydrogen peroxide dynamics in vivo. *Anal. Chem.* **90**, 888–895 (2018).
83. Smith, S. K. et al. Simultaneous voltammetric measurements of glucose and dopamine demonstrate the coupling of glucose availability with increased metabolic demand in the rat striatum. *ACS Chem. Neurosci.* **8**, 272–280 (2017).
84. Lugo-Morales, L. Z. et al. Enzyme-modified carbon-fiber microelectrode for the quantification of dynamic fluctuations of nonelectroactive analytes using fast-scan cyclic voltammetry. *Anal. Chem.* **85**, 8780–8786 (2013).
85. Burmeister, J. J., Palmer, M. & Gerhardt, G. A. L-lactate measures in brain tissue with ceramic-based multisite microelectrodes. *Biosens. Bioelectron.* **20**, 1772–1779 (2005).
86. Burmeister, J. J. et al. Ceramic-based multisite microelectrode arrays for simultaneous measures of choline and acetylcholine in CNS. *Biosens. Bioelectron.* **23**, 1382–1389 (2008).
87. Day, B. K., Pomerleau, F., Burmeister, J. J., Huettl, P. & Gerhardt, G. A. Microelectrode array studies of basal and potassium-evoked release of L-glutamate in the anesthetized rat brain. *J. Neurochem.* **96**, 1626–1635 (2006).
88. Ngernsutivorakul, T., White, T. S. & Kennedy, R. T. Microfabricated probes for studying brain chemistry: a review. *ChemPhysChem* **19**, 1128–1142 (2018).
89. Zestos, A. G. & Kennedy, R. T. Microdialysis coupled with LC-MS/MS for in vivo neurochemical monitoring. *AAPS J.* **19**, 1284–1293 (2017).
90. Wong, J.-M. T. et al. Benzoyl chloride derivatization with liquid chromatography-mass spectrometry for targeted metabolomics of neurochemicals in biological samples. *J. Chromatogr. A* **1446**, 78–90 (2016).
91. Rogers, M. L. et al. Simultaneous monitoring of potassium, glucose and lactate during spreading depolarization in the injured human brain: proof of principle of a novel real-time neurochemical analysis system, continuous online microdialysis. *J. Cereb. Blood Flow Metab.* **37**, 1883–1895 (2017).
92. Papadimitriou, K. I. et al. High-performance bioinstrumentation for real-time neuroelectrochemical traumatic brain injury monitoring. *Front. Hum. Neurosci.* **10**, 212 (2016).

93. Wang, M., Roman, G. T., Schultz, K., Jennings, C. & Kennedy, R. T. Improved temporal resolution for in vivo microdialysis by using segmented flow. *Anal. Chem.* **80**, 5607–5615 (2008).
94. Lee, W. H. et al. Microfabrication and in vivo performance of a microdialysis probe with embedded membrane. *Anal. Chem.* **88**, 1230–1237 (2016).
95. Quiroz, C. et al. Local control of extracellular dopamine levels in the medial nucleus accumbens by a glutamatergic projection from the infralimbic cortex. *J. Neurosci.* **36**, 851–859 (2016).
96. Al-Hasani, R. et al. In vivo detection of optically-evoked opioid peptide release. *eLife* **7**, e36520 (2018).
97. Alexander, G. M. et al. Remote control of neuronal activity in transgenic mice expressing evolved G protein-coupled receptors. *Neuron* **63**, 27–39 (2009).
98. Vardy, E. et al. A new DREADD facilitates the multiplexed chemogenetic interrogation of behavior. *Neuron* **86**, 936–946 (2015).
99. Hüll, K., Morstein, J. & Trauner, D. In vivo photopharmacology. *Chem. Rev.* **118**, 10710–10747 (2018).
100. Broichhagen, J., Frank, J. A. & Trauner, D. A roadmap to success in photopharmacology. *Acc. Chem. Res.* **48**, 1947–1960 (2015).
101. Banala, S. et al. Photoactivatable drugs for nicotinic optopharmacology. *Nat. Methods* **15**, 347–350 (2018).
102. Dong, M., Babalhavaeji, A., Samanta, S., Beharry, A. A. & Woolley, G. A. Red-shifting azobenzene photoswitches for in vivo use. *Acc. Chem. Res.* **48**, 2662–2670 (2015).
103. Wagner, N., Stephan, M., Höglinger, D. & Nadler, A. A click cage: organelle-specific uncaging of lipid messengers. *Angew. Chem. Int. Ed. Engl.* **57**, 13339–13343 (2018).
104. Nadler, A. et al. Exclusive photorelease of signalling lipids at the plasma membrane. *Nat. Commun.* **6**, 10056 (2015).
105. Yang, G. et al. Genetic targeting of chemical indicators in vivo. *Nat. Methods* **12**, 137–139 (2015).
106. Shields, B. C. et al. Deconstructing behavioral neuropharmacology with cellular specificity. *Science* **356**, eaaj1682 (2017).
107. Berry, M. H. et al. Restoration of patterned vision with an engineered photoactivatable G protein-coupled receptor. *Nat. Commun.* **8**, 1862 (2017).
108. Levitz, J. et al. Dual optical control and mechanistic insights into photoswitchable group II and III metabotropic glutamate receptors. *Proc. Natl Acad. Sci. USA* **114**, E3546–E3554 (2017).
109. Takemoto, K. et al. Optical inactivation of synaptic AMPA receptors erases fear memory. *Nat. Biotechnol.* **35**, 38–47 (2017).
110. Tischbirek, C., Birkner, A., Jia, H., Sakmann, B. & Konnerth, A. Deep two-photon brain imaging with a red-shifted fluorometric Ca^{2+} indicator. *Proc. Natl Acad. Sci. USA* **112**, 11377–11382 (2015).
111. Deal, P. E., Kulkarni, R. U., Al-Abdullatif, S. H. & Miller, E. W. Isomerically pure tetramethylrhodamine voltage reporters. *J. Am. Chem. Soc.* **138**, 9085–9088 (2016).
112. Martineau, M. et al. Semisynthetic fluorescent pH sensors for imaging exocytosis and endocytosis. *Nat. Commun.* **8**, 1412 (2017).
113. Sallin, O. et al. Semisynthetic biosensors for mapping cellular concentrations of nicotinamide adenine dinucleotides. *eLife* **7**, e32638 (2018).
114. Shin, H. et al. Neural probes with multi-drug delivery capability. *Lab Chip* **15**, 3730–3737 (2015).
115. Uguz, I. et al. A microfluidic ion pump for in vivo drug delivery. *Adv. Mater.* **29**, 1701217 (2017).
116. Schubert, R. et al. Virus stamping for targeted single-cell infection in vitro and in vivo. *Nat. Biotechnol.* **36**, 81–88 (2018).
117. Jackman, S. L. et al. Silk fibroin films facilitate single-step targeted expression of optogenetic proteins. *Cell Rep.* **22**, 3351–3361 (2018).
118. Chan, K. Y. et al. Engineered AAVs for efficient noninvasive gene delivery to the central and peripheral nervous systems. *Nat. Neurosci.* **20**, 1172–1179 (2017).
119. Zhao, Z. et al. Nanoelectronic coating enabled versatile multifunctional neural probes. *Nano Lett.* **17**, 4588–4595 (2017).
120. Dagdeviren, C. et al. Miniaturized neural system for chronic, local intracerebral drug delivery. *Sci. Transl. Med.* **10**, eaan2742 (2018).
121. Kampasi, K. et al. Fiberless multicolor neural optoelectrode for in vivo circuit analysis. *Sci. Rep.* **6**, 30961 (2016).
122. Kampasi, K. et al. Dual color optogenetic control of neural populations using low-noise, multishank optoelectrodes. *Microsyst. Nanoeng.* **4**, 10 (2018).
123. Minev, I. R. et al. Electronic dura mater for long-term multimodal neural interfaces. *Science* **347**, 159–163 (2015).
124. Petit-Pierre, G., Bertsch, A. & Renaud, P. Neural probe combining microelectrodes and a droplet-based microdialysis collection system for high temporal resolution sampling. *Lab Chip* **16**, 917–924 (2016).
125. Lee, W. et al. Transparent, conformable, active multielectrode array using organic electrochemical transistors. *Proc. Natl Acad. Sci. USA* **114**, 10554–10559 (2017).
126. Park, D. W. et al. Electrical neural stimulation and simultaneous in vivo monitoring with transparent graphene electrode arrays implanted in GCaMP6f mice. *ACS Nano* **12**, 148–157 (2018).
127. Thunemann, M. et al. Deep 2-photon imaging and artifact-free optogenetics through transparent graphene microelectrode arrays. *Nat. Commun.* **9**, 2035 (2018).
128. Kuzum, D. et al. Transparent and flexible low noise graphene electrodes for simultaneous electrophysiology and neuroimaging. *Nat. Commun.* **5**, 5259 (2014).
129. Jiang, Y. et al. Rational design of silicon structures for optically controlled multiscale biointerfaces. *Nat. Biomed. Eng.* **2**, 508–521 (2018).
130. Kilias, A. et al. Optogenetic entrainment of neural oscillations with hybrid fiber probes. *J. Neural Eng.* **15**, 056006 (2018).
131. Rein, M. et al. Diode fibres for fabric-based optical communications. *Nature* **560**, 214–218 (2018).
132. Qu, Y. et al. Superelastic multimaterial electronic and photonic fibers and devices via thermal drawing. *Adv. Mater.* **30**, e1707251 (2018).
133. Grena, B. et al. Thermally-drawn fibers with spatially-selective porous domains. *Nat. Commun.* **8**, 364 (2017).
134. Montgomery, K. L., Iyer, S. M., Christensen, A. J., Deisseroth, K. & Delp, S. L. Beyond the brain: optogenetic control in the spinal cord and peripheral nervous system. *Sci. Transl. Med.* **8**, 337rv5 (2016).
135. Shemesh, O. A. et al. Temporally precise single-cell-resolution optogenetics. *Nat. Neurosci.* **20**, 1796–1806 (2017).
136. Berlin, S. et al. Photoactivatable genetically encoded calcium indicators for targeted neuronal imaging. *Nat. Methods* **12**, 852–858 (2015).
137. Kandel, E. R. et al. *Principles of Neural Science* 5th edn (McGraw-Hill Education/Medical, 2012).
138. Pomeroy, J. E., Nguyen, H. X., Hoffman, B. D. & Bursac, N. Genetically encoded photoactuators and photosensors for characterization and manipulation of pluripotent stem cells. *Theranostics* **7**, 3539–3558 (2017).

Acknowledgements

This work was supported in part by the National Institute of Neurological Disorders and Stroke (5R01NS086804), the National Institutes of Health BRAIN Initiative (1R01MH111872), the National Science Foundation through the Center for Materials Science and Engineering (DMR-1419807) and the Center for Neurotechnology (EEC-1028725), and by the McGovern Institute for Brain Research at MIT.

Author contributions

J.A.F. and M.-J.A. researched data for the article. J.A.F., M.-J.A. and P.A. discussed the article scope and wrote the manuscript.

Competing interests

The authors declare no competing interests.

Additional information

Reprints and permissions information is available at www.nature.com/reprints.

Correspondence should be addressed to P.A.

Publisher's note: Springer Nature remains neutral with regard to jurisdictional claims in published maps and institutional affiliations.